re-BUS

You have downloaded a document from
RE-BUŚ
repository of the University of Silesia in Katowice

Title: Glass Transition Dynamics of Poly(phenylmethylsiloxane) Confined within Alumina Nanopores with Different Atomic Layer Deposition (ALD) Coatings

Author: Roksana Winkler, Katarzyna Chat, Aparna Beena Unni, Mateusz Dulski, Karolina Adrjanowicz [i in.]

Citation style: Winkler Roksana, Chat Katarzyna, Unni Aparna Beena, Dulski Mateusz, Adrjanowicz Karolina [i in.]. (2022). Glass Transition Dynamics of Poly(phenylmethylsiloxane) Confined within Alumina Nanopores with Different Atomic Layer Deposition (ALD) Coatings. "Macromolecules" (2022), vol. 13, art. no 860281. DOI: 10.1021/acs.macromol.2c00311

Uznanie autorstwa - Licencja ta pozwala na kopiowanie, zmienianie, rozprowadzanie, przedstawianie i wykonywanie utworu jedynie pod warunkiem oznaczenia autorstwa.

UNIWERSYTET ŚLĄSKI W KATOWICACH
Biblioteka Uniwersytetu Śląskiego
Ministerstwo Nauki i Szkolnictwa Wyższego

Macromolecules

pubs.acs.org/Macromolecules

Article

Glass Transition Dynamics of Poly(phenylmethylsiloxane) Confined within Alumina Nanopores with Different Atomic Layer Deposition (ALD) Coatings

Roksana Winkler,* Katarzyna Chat, Aparna Beena Unni, Mateusz Dulski, Magdalena Laskowska, Lukasz Laskowski, and Karolina Adrjanowicz*

Cite This: https://doi.org/10.1021/acs.macromol.2c00311

Read Online

ACCESS | Metrics & More | Article Recommendations | Supporting Information

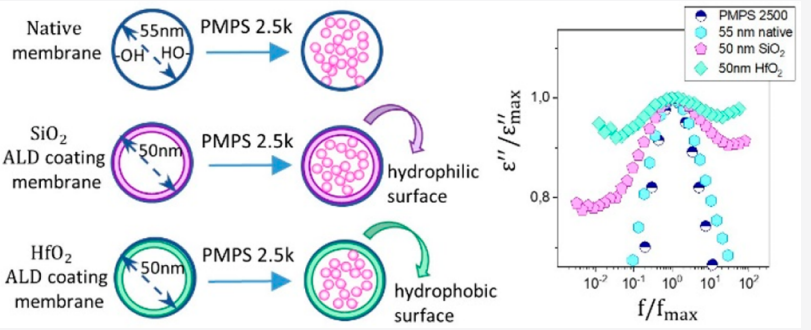

ABSTRACT: Dielectric spectroscopy (DS) and differential scanning calorimetry (DSC) were employed to study the effect of changes in the surface conditions on the segmental dynamics of poly(phenylmethylsiloxane) confined in alumina nanopores (AAO). The inner surface of the pores was modified by using the atomic layer deposition technique. Coated membranes include 5 nm thick layers of hafnium oxide, titanium oxide, and silicon oxide, exhibiting different wetting properties. Modification of the surface conditions dramatically affects the interfacial interactions between the polymer and confining surface. The interfacial energy calculations indicate a decrease of γ_{SL} value from 18.7 mN/m in SiO_2-coated to 0.5 mN/m in HfO_2-coated nanopores. The results of the dielectric relaxation study demonstrate that the segmental relaxation time of confined PMPS 2.5k depends on the thermal treatment protocol and the hydrophilic/hydrophobic character of the pore walls. From calorimetric measurements, we found that the two glass transitions events are still observed, even in the absence of strong interfacial interactions. Values of both T_gs do not depend strongly on the chemical nature of the surface. In this way, changes in the glass-transition behavior of the tested polymer confined in ALD-coated nanopores cannot be rationalized in terms of the polymer/substrate interfacial energy. Eliminating strongly adhered surfaces does not eliminate the puzzling two-T_gs effect seen in cylindrical nanopores.

INTRODUCTION

In nanotechnology, it is essential to understand the changes that take place with the polymer materials under geometrical confinement. Modification of the polymer's physical and chemical properties at the nanoscale level results in them being successfully used in numerous fields of modern technology.[1−7] Apart from that it, has been demonstrated that nanoconfinement has an enormous impact on the glass transition dynamics.[8,9]

The glass transition dynamics of the polymer materials subjected to nanometric confinement is—in many cases—notably different from the bulk. It has been recognized that this behavior depends on several factors, which include the finite size effect, interfacial interactions,[10] conformational changes,[11−14] free volume,[15,16] negative pressure effects,[17,18] and surface properties (including the impact of the roughness,[19] silanization,[20] or polarity[21]). Thus, lowering the pore diameter or modifying the surface interactions typically changes the glass transition temperature value.[22−29] In addition, the thermal history of the sample also influences the glass transition dynamics.[30−33] For example, it can broaden the shape of the segmental relaxation and decrease its dielectric strength.[8,34,35] Apart from that, the properties of the confined material can change due to interactions with the constraining environment.[8,35−38]

Another important aspect of polymer dynamics in confined space is the nonequilibrium effect. The literature data indicate

Received: February 11, 2022
Revised: March 23, 2022

ACS Publications

© XXXX The Authors. Published by American Chemical Society

that soft matter under nanoconfinement can remain in this state for a very long time.[39] On the other hand, it was also observed that the long-time annealing experiment could remove the confinement effect, and the polymer dynamics can recover some of its bulk features.[20,30,39−42] For example, in thin polymer films, prolonged annealing slows down the dynamics[42] and affects the conformation of the polymer chains placed near the substrate due to irreversible adsorption.[10,16,40,41,43−45] The out-of-equilibrium behavior is also seen for glass-forming materials confined in nanopores (2D confinement).[11,30−33] Numerous studies indicate that upon annealing the polymer chain packing density changes, slowing down the segmental dynamics; therefore, the confined material can recover—at least partially—its bulk properties.[30,33] However, the enormous impact on the glass transition dynamics in the confined state is also due to the surface interactions.[9,20,28,46−51] In short, the outcome polymer dynamics in nanoscale confinement is considered as the outcome of the balance between finite size and surface effects.[8,52−54]

The surface effect arises from the interactions between guest molecules and the hard-confining walls of the nanopores. Generally, this effect in native nanopores, which has a hydrophilic profile, leads to a two-layer scenario. We differentiate the interfacial layer, where the molecular mobility closer to the pore walls is slowed down,[55] and the core fraction of the molecules with enhanced mobility.[8,56−58] The primary mechanism of the interactions between the sample and the pore walls is hydrogen bonding, which can be removed by the chemical substitution of the hydroxyl groups anchored to the surface via the silanization process. Previous investigations show that the glass transition temperature[49] and the hydrophilic character of the inner pore walls[9,49,50,59,60] change when replacing the hydroxyl groups at the surface by using various silane agents.[49] Furthermore, the formation of the core−shell structure in surface-modified nanopores seems to depend on the cooling rate.[46] Some previous reports suggest that silanization can partially or entirely eliminate the enhanced glass transition dynamics under confinement.[60−64] On the other hand, decreasing the pore diameter makes this effect more noticeable.[61,63]

Changes in the glass transition dynamics caused by silanization depend on the silane agent. Some silane agents are more effective in creating homogeneous hydrophobic surfaces on alumina surfaces than others. This, in turn, might have a significant impact on the temperature evolution of the segmental relaxation time. These findings were discussed in our previous work, where we used alumina membranes coated with chlorotrimethylsilane (ClTMS) and (3-aminopropyl)-trimethoxysilane (APTMOS).[20] As a matter of fact, more precise control over surface conditions is when using a phosphonic acid functionalization. This strategy can involve, for example, the separation of highly polar phosphoric units by a controlled number of nonpolar spacers. Interestingly, our data indicate that in such a case precise control over surface polarity might prevent the formation of the interlayer between the adsorbed layer and core volume observed in native alumina nanopores.[21]

Apart from that, atomic layer deposition might shed new light on the role of surface conditions in determining the glass transition dynamics in nanopore confinement. ALD is a modern thin film growth technique that allows controlling pore wall composition and the pore diameter.[65,66] ALD coating of AAO nanopores provides a compositionally uniform surface and modifies the hydroxyl groups present on the surface. More specifically, Al_2O_3 layers remove isolated hydroxyl groups and keep only hydrogen-bonded hydroxyl groups. Therefore, ALD alumina coatings are free of defects.[67] Chat et al. have shown that for the molecular liquid dimethyl phthalate, confined in alumina nanopores with different ALD coatings, changes in the hydrophilicity/hydrophobicity of the surface do not affect significantly the molecular dynamics and the value of glass transition temperatures for both interfacial and core layers as compared to the native nanopores.[68] On the other hand, modification of the hydrophilic−hydrophobic character of the pores can be used to control the crystallization tendency. In contrast, for the strongly polar molecular liquid S-Methoxy-PC, confined within alumina nanopores with a hafnium oxide coating, it has been demonstrated that the molecular movements slow down.[69] In both cases, it was observed that when the surface was more hydrophobic, the α-relaxation peak broadened.

In this work, we report the effect of changes in the surface condition on the glass transition dynamics of poly(phenylmethylsiloxane) (PMPS) confined within cylindrical ALD-coated alumina nanopores. For this purpose, we have performed dielectric spectroscopy and differential scanning calorimetry. We chose a 5 nm thick oxide coating of hafnium oxide (HfO_2), titanium oxide (TiO_2), and silicon oxide (SiO_2). They show different surface properties, from hydrophobic to more hydrophilic. Furthermore, they are suitable components for nanotechnology applications. PMPS was chosen for this study because even a minimal frustration in the packing density significantly affects its glass transition dynamics in confined space. In line with the previous study results,[20,21] we show that changes in the surface character do not erase the confinement effect. Therefore, two glass-transition events are still detected in DSC thermograms. This is an astonishing finding, especially by taking into account the exceptionally low value of the interfacial energy between PMPS and HfO_2 ($\gamma_{SL} \sim 0.5$ mN/m). In turn, the analysis of Raman spectra (shown in the Supporting Information) suggests that the observed structural modifications within PMPS 2.5k chain come primarily from the confinement effect. Changes in the surface condition result only in the higher structural modifications within siloxane- and aromatic-related bands. There are no other noticeable differences. The results of this study, together with the previous one, keep the question open on whether the presence of two glass transition events seen in cylindrical nanopores is indeed related to the interactions of the confined sample with the rigid walls or some other phenomena taking place close to the surface.

What this study brings new, compared to the previous work, is also that the inner surface of the pores is modified by the chemical deposition of (hard) inorganic layers onto it. In contrast, the typical modification of the nanopore surface conditions involves silanization (soft-organic coatings). It should also be highlighted that the methodology of the present work assumes keeping the same tested polymer, cylindrical pore geometry, and its size. This idea has a more in-depth meaning because the only variable parameter is the surface properties of nanoporous material, while typically, different glass-forming materials are embedded within the native nanoporous alumina templates. As will be demonstrated in the further part of this paper, this has allowed us to evaluate changes in the polymer/substrate interfacial energy and its role

https://doi.org/10.1021/acs.macromol.2c00311
Macromolecules XXXX, XXX, XXX−XXX

in determining segmental dynamics in confined space from a completely different point of view. Apart from that, the results show that the ALD technique is a very effective strategy to tune the polymer−substrate interactions in confined space in an extensive range. By knowing how the polymer material behaves in the presence of various surface coatings, either organic or inorganic, we can facilitate our knowledge on nanoscale phenomena to modulate different properties of soft matter systems and further development.

EXPERIMENTAL SECTION

Materials. Poly(phenylmethylsiloxane), labeled in the text as PMPS 2.5k, was purchased from Polymer Source Inc. (Canada). The molecular weight of the tested material is M_n = 1800, and its polydispersity index (PDI) = 1.4. The chemical structure of PMPS can be found in Figure 1. The number of monomer subunits does not exceed 20, so it can also be considered more formally as an oligomer. The sample was provided as a clear, viscous, transparent liquid and used without further purification. Usually, T_g determined from dielectric relaxation studies is defined as a temperature at which segmental relaxation time τ_α = 100 s. However, to be consistent with the previous literature data, we have defined the glass transition temperature of PMPS by using τ_α = 1 s. The value of T_g determined from the dielectric measurements (DS) of bulk PMPS 2.5k is T_g = 230 K.[20,70] In turn, based on differential scanning calorimetry (DSC) data, the reported value of T_g = 230.3 K.[20,70] As typically observed for polymer materials, the value of glass transition temperature for PMPS increases with the molecular weight.[71−75] Alexandris et al. studied PMPS with M_n = 2200 and PDI 1.28 and found T_g = 229 K (DS) and T_g = 228 K (DSC),[75] which are in good agreement with our results.

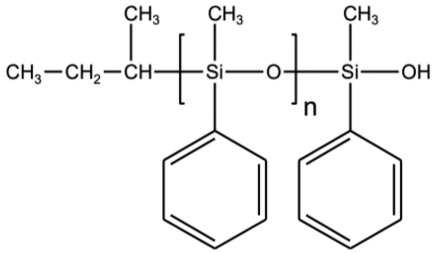

Figure 1. Chemical structure of poly(phenylmethylsiloxane), used in this study.

AAO Nanopores with ALD Coatings. We have used anodized aluminum oxide (AAO) membranes with different ALD coatings (pore diameter of 25, 50, and 100 nm, pore depth 50 μm) that were fabricated by Inredox (USA). The membranes are composed of uniform arrays of unidirectional and non-cross-linking nanopores. More details about the ALD technology applied to AAO nanopores can be found on the supplier's website. The diameter of alumina membranes with different ALD coatings is 10 mm, and its thickness is 50 μm. We have used membranes with 5 nm thick layers of the following oxides: HfO_2, SiO_2, and TiO_2. In this way, the actual pore diameter should be reduced from 25, 50, and 100 nm to respectively 15, 40, and 90 nm. The declared porosity of nanopores used in this study varies within 20−24% and the pore density 10^9−10^{10} cm^{-2}. Independently, we have performed N_2 adsorption/desportion analysis to confirm the quality of supplied membranes. SEM images were also taken to identify the surface morphology. These results can be found in the Supporting Information.

Before infiltration, the membranes were dried at 353 K in a vacuum oven for 8 h to remove all volatile impurities from the nanochannels. We have not increased above this temperature because HfO_2 might convert to another crystalline phase at high temperatures, while TiO_2 is not stable upon prolonged annealing at temperatures close to 500 °C.[67] Before and after infiltration, all the membranes were weighted. Then, the PMPS 2.5k were placed on the top of the AAO membranes, and the entire system was kept at T = 308 K under vacuum for 2 weeks. This allows the capillary flow. The filling was completed when the mass of the membrane ceased to increase. In the end, the membranes were dried by using delicate dust-free tissues. The degree of membrane filling was estimated by using two approaches that employ either membrane porosity or pore density. The details can be found in the Supporting Information. Typically, the polymer mass inside 50 nm AAO nanopores with various ALD coatings varies from 0.7 mg (for HfO_2 and TiO_2 layers) to 1.1 mg (for SiO_2 layers). Thus, the determined percentage of filling was more than 90%.

Methods. *Contact Angle Goniometry.* The sessile drop technique using a JC2000D contact angle tester under ambient humidity and temperature was employed to measure the contact angle. Ultrapure water, formamide, DMSO, ethylene glycol, and glycerol were used as tests liquids. The contact angle was measured immediately after dropping and next with the interval of 5 s to check the evolution of CA. We did not observe any significant changes; thus, the first measurement was taken under consideration. We have used 5 μL of solvent in each drop. The average value was obtained as the average of several independent measurements.

Dielectric Spectroscopy (DS). Dielectric spectroscopy measurements for bulk and nanopore-confined PMPS were made with a Novocontrol Alpha frequency analyzer. For the bulk sample, we use a standard plate−plate electrode of 20 mm in diameter separated by a 50 μm Teflon spacer. A Teflon spacer was used to maintain fixed gap between the electrodes. The ALD-coated alumina membranes filled with the investigated polymer were placed between two round stainless steel electrodes with a diameter of 10 mm. Bulk and alumina membranes with ALD coatings were measured as a function of temperature in the frequency range from 10^{-2} to 10^6 Hz. The Quatro system controls the temperature with stability better than 0.1 K. The complex dielectric permittivity $\varepsilon^* = \varepsilon' - i\varepsilon''$, where ε' is the real and ε'' is the imaginary part, was recorded on (i) slow cooling with a rate of 0.2 K/min from 293 to 219 K and (ii) slow heating from 219 to 293 K with ∼0.2 K/min after quenching (∼10−13 K/min) in the glassy state. We use two different thermal protocols to verify the effect of thermal protocol on the confined polymer dynamics. For this reason we use either very slow cooling from room temperature or rapid quenching before measurements on subsequent heating.

It should be remembered that the dielectric data measured in this way show a nontrivial combination of two mixing signals coming from confined PMPS 2.5k and porous alumina. Thus, before any analysis is performed, correction of the raw data is needed. The problem of heterogeneous dielectric systems, such as alumina nanopores filled with the studied polymer, can be considered as a system of two capacitors connected parallelly in an electric circuit. In such a way, the permittivities of the components—after being weighted by the respective volume fractions—are additive. However, the additional air-gap contribution must be considered when the nanopores are not entirely filled with the polymer. In this case, the system can be modeled as series capacitances. This has been demonstrated recently for alumina confined ionic liquid samples.[76,77] Experimentally, in the dielectric spectra, the air-gaps (electrode blocking), if large enough, may be responsible for the presence of the additional low-frequency relaxation and deviate the α-relaxation to higher frequencies.[78,79] However, this is not the case in this study. As demonstrated in the Supporting Information, the correction, which includes the contribution coming from the matrix and incomplete pore filling/air gaps (∼10%) with the tested polymer, modifies only the intensity of the dielectric permittivity while not the position of the segmental relaxation or either its shape. In the previous study, we have also ended up with the same finding.[20,21] Nevertheless, one should bear in mind that such correction is mandatory before evaluating the conductivity behavior of ionic liquids in nanopore confinement or when the air-gap contribution is more dominant.

Differential Scanning Calorimetry (DSC). A Mettler-Toledo DSC apparatus was used to perform calorimetric measurements. This system has a liquid nitrogen cooling accessory and an HSS8 ceramic sensor (heat flux sensor with 120 thermocouples). Indium and zinc standards are used for temperature and enthalpy calibrations.

https://doi.org/10.1021/acs.macromol.2c00311
Macromolecules XXXX, XXX, XXX−XXX

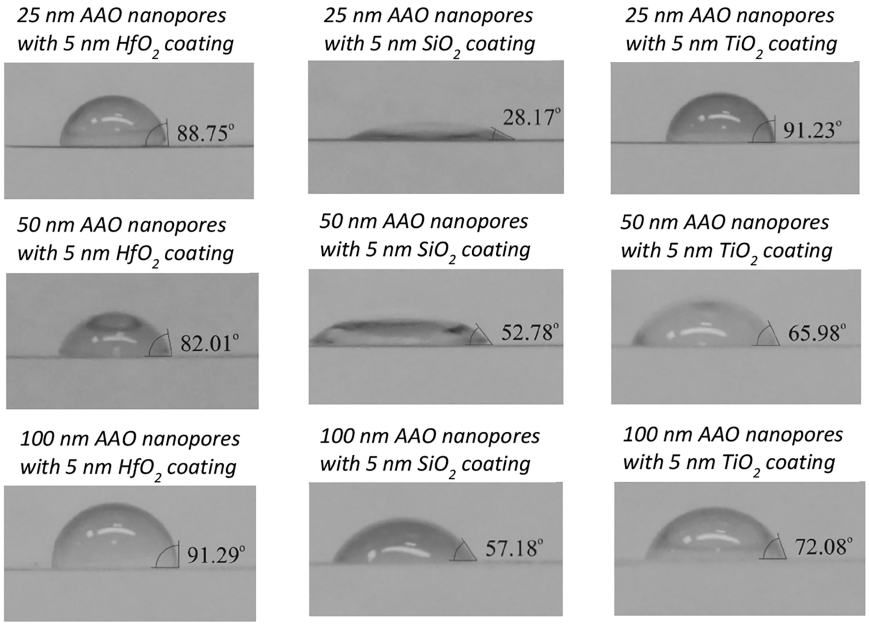

Figure 2. Contact angle measurements for the AAO nanopores with different sizes and ALD coatings measured for water as a test liquid.

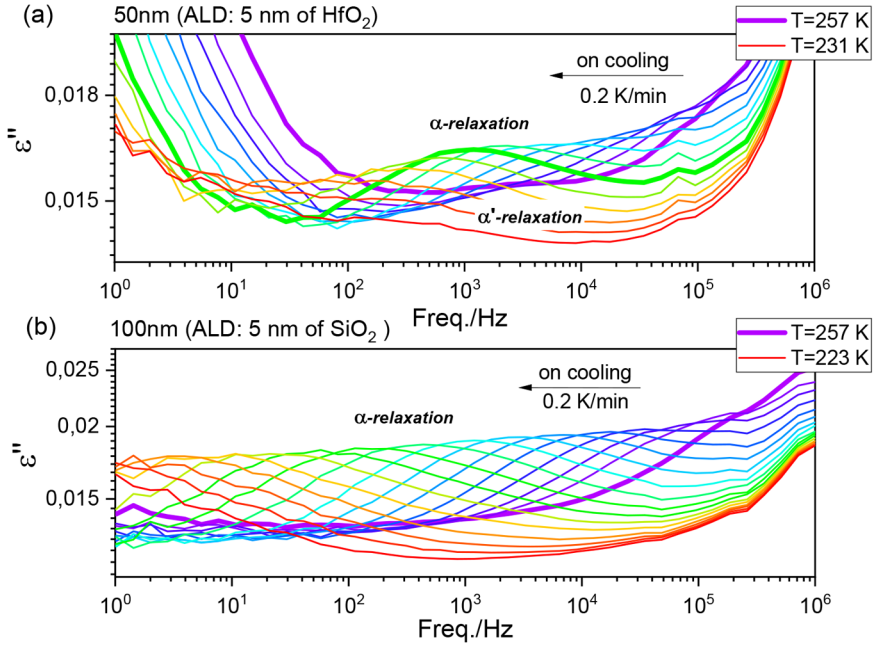

Figure 3. Dielectric loss spectra of PMPS 2.5k recorded in (a) 50 nm alumina nanopores with 5 nm HfO_2 coating and (b) 100 nm alumina nanopores with 5 nm SiO_2 coating. The spectra for the polymer−matrix composite materials were measured upon cooling with a rate of 0.2 K/min.

Crucibles with prepared samples (bulk or crushed alumina membranes containing confined PMPS) were sealed and cooled to 183 K with a 2 K/min rate inside the DSC machine. Then, calorimetric data were recorded on heating with a rate of 10 K/min in the temperature range from 183 to 293 K. From heat flow data, T_g was defined as the temperature corresponding to the midpoint inflection the extrapolated transition curve at the onset and end.

RESULTS AND DISCUSSION

We start our investigation by demonstrating the contact angle results for AAO nanopores with different ALD coatings and pore sizes. In this way, the nanoporous templates were characterized by their hydrophilic/hydrophobic character. We want to note that the inner surface of the walls for each of the membranes was covered by a 5 nm thick ALD coating of either HfO_2, SiO_2, and TiO_2; consequently, the actual pore diameter is reduced by 10 nm. The contact angle results measured for water as a test liquid are presented in Figure 2. Herein, it should be noted that the surface has hydrophilic properties when the value of the contact angle is lower than 90°. The surface becomes hydrophobic with the increasing contact angle (above 90°). The literature data demonstrate that the native nanopores exhibit hydrophilic properties.[20,80]

In our case, the nanopores with SiO_2 and TiO_2 have a more hydrophilic surface (especially SiO_2), unlike the HfO_2

https://doi.org/10.1021/acs.macromol.2c00311
Macromolecules XXXX, XXX, XXX−XXX

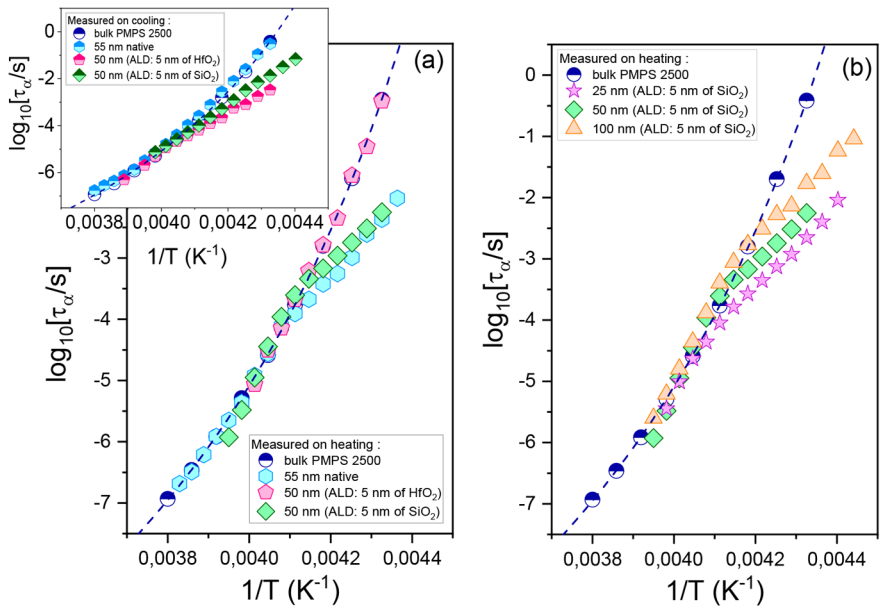

Figure 4. (a) Comparison of the temperature evolution of the segmental relaxation time for PMPS 2.5k confined to AAO nanopores with native (pore sizes 55 nm) and ALD-coated (actual pore size 40 nm) walls. The data were measured by using two different thermal protocols. The main panel show α-relaxation times recorded on slow heating prior to the sample was quenched from the room temperature to the temperature region deep in the glassy state. The inset shows the temperature dependence of the α-relaxation time measured on cooling from the room temperature with the rate of ~0.5 K/min. (b) Evolution of the segmental relaxation time for PMPS 2.5k confined to AAO membranes with SiO_2 ALD coating as a function of different pore sizes. Data were measured on heating. The blue line represents the fitted VFT function to the bulk data. The results for the bulk polymer were shown as a reference.

membranes, which are rather hydrophobic. Former experimental work confirms the hydrophilic nature of silicon[81] and titanium oxides[82,83] and the hydrophobic properties of hafnium oxide coatings.[84−86] In our previous study, functionalization was prepared by adjusting the proportion between highly polar phosphoric units and nonpolar spacers. In such a case, we have discovered that the hydrophobic properties of the surface increase with increasing the number of nonpolar units per single polar group.[21] Furthermore, literature data suggest that the glass transition dynamics under nanoconfinement might depend on the hydrophilicity/hydrophobicity of the inner pore walls.[9,20,49,68,69]

A dielectric relaxation study was performed to investigate the glass-transition dynamics of PMPS 2.5k in confined geometry. From our previous study of PMPS 2.5k, we know that for the bulk material in the dielectric loss spectra we can distinguish α'-, α-, and β-relaxation processes.[70] The α-relaxation is due to segmental mobility, while the β-relaxation process describes more local motions, strongly linked to the structural relaxation. On the other hand, α'-relaxation is due to the sub-Rouse mode. Figure 3a presents representative raw dielectric loss spectra for the studied polymer embedded within 50 nm pore with HfO_2 coating, while Figure 3b shows the 100 nm pore with SiO_2 coating, as measured at different temperatures. Unfortunately for TiO_2-coated nanopores, it was impossible to observe any relaxation process in BDS because TiO_2 behaves like a semiconductor with high electron mobility. The considerable conductivity of the system covers the relaxations processes, while SiO_2 and HfO_2 are insulator materials where the electron mobility is lower.[87] The dielectric spectra of (i) unfilled membranes with different ALD coatings and (ii) PMPS 2.5k confined within 25 and 50 nm membranes can be found in the Supporting Information.

We have observed the prominent α-relaxation process. Its intensity decreases at lower temperatures for all nanopore-confined samples with different ALD coatings. The α'-relaxation process was also detected. Nevertheless, we have excluded it from further consideration due to very weak intensity compared to segmental relaxation. By comparison of the dielectric loss spectra for PMPS 2.5k confined in nanopores with various surface modifications, it is noticeable that the secondary β-relaxation process disappears. The same feature was already detected for PMPS 27.7k determined in AAO nanopores.[74] The suppression of the β-relaxation under confinement can be connected with the interactions between host and guest system and the changes in density. Each of these factors may affect the geometry and conformation of the molecules and the variation in the angle of dipole moment vibrations.

The dielectric loss spectra were analyzed by using the Havriliak−Negami (HN) function[88]

$$\varepsilon^*(\omega) = \varepsilon_\infty + \frac{\Delta\varepsilon}{[1 + (i\omega\tau_{HN})^a]^b} + \frac{\sigma_0}{i\omega\varepsilon_0} \quad (1)$$

where $\Delta\varepsilon$ is the dielectric strength, ε_∞ is the high-frequency limit of the permittivity, a and b are the shape parameters, σ_0 is the dc conductivity, τ_{HN} denotes the relaxation time, and ω is the angular frequency ($\omega = 2\pi f$). In HN function, the characteristic time constant, τ_{HN}, is related to the maximum of loss peak frequency f_{max} by the following relation:[89]

$$f_{max} = \frac{1}{\tau_{HN}}\left[\sin\left(\frac{a\pi}{2 + 2b}\right)\right]^{1/a}\left[\sin\left(\frac{ab\pi}{2 + 2b}\right)\right]^{-1/a} \quad (2)$$

The collected dielectric loss spectra were analyzed for the α-process by using the standard fitting procedure. By calculating $\tau_{max} = 1/(2\pi f_{max})$, we determined the relaxation times. In this

https://doi.org/10.1021/acs.macromol.2c00311
Macromolecules XXXX, XXX, XXX−XXX

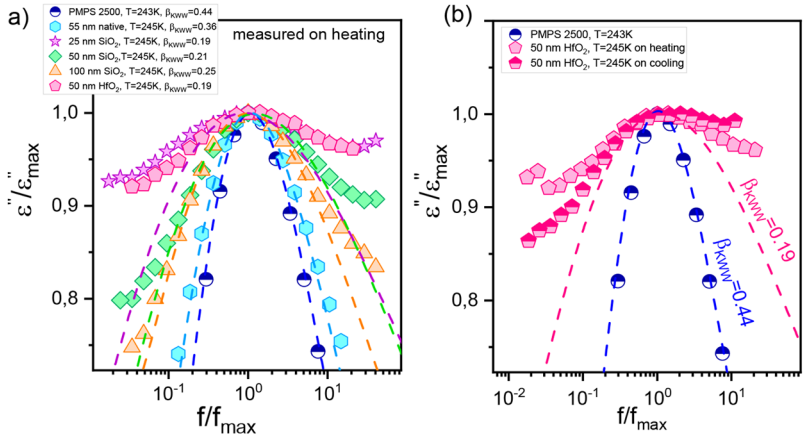

Figure 5. Comparison of the shape of the α-relaxation peak for PMPS 2.5k confined to AAO nanopores: (a) with native and ALD-modified pore surface and for different diameters of the nanopores; (b) with HfO_2 ALD coating as measured using two different thermal protocols. The bulk spectrum collected at T = 243 K was used as a reference. Dashed lines are fits to the KWW function.

way, we obtained the temperature dependences of the α-relaxation time for PMPS 2.5k confined in AAO nanopores with different ALD coatings and different pore sizes which are presented in Figures 4a and 4b, respectively.

As can be seen, the segmental process for bulk polymer exhibits Vogel−Fulcher−Tammann (VFT) behavior, which can be approximated applying the following equation[90−92]

$$\tau_\alpha = \tau_\infty \exp\left(\frac{B}{T - T_0}\right) \tag{3}$$

where τ_∞ is the high-temperature limit of the relaxation time, B is the activation parameter, and T_0 is the "ideal" glass temperature, often called the Vogel temperature. As can be seen, at higher temperatures, the nanopores with different ALD coating follow bulk dependence. Then, with decreasing the temperature, the characteristic deviation in $\tau_\alpha(T)$ appears. This observation agrees with our previous results for PMPS 2.5k confined in AAO nanopores with chemically modified surfaces.[20,21] Similar behavior was also reported for many other glass-forming substances under nanoconfinement.[18,20,56−58,93,94] Such deviation of the $\tau_\alpha(T)$ from the bulk is often related to the presence of two fractions of molecules, i.e., the interfacial and core layers. In each layer, the molecules have different mobility. In the interfacial layer, the molecules strongly interacting with the walls of the pores are characterized by slower mobility, while in the core, the mobility of molecules is faster.[37,57] Therefore, the interfacial mobility vitrifies as higher temperature, while the molecules in the core at slower. In many cases, it is impossible to observe the dynamics associated with the interfacial layer on dielectric loss spectra. Nevertheless, by combining dielectric and calorimetric results, it was demonstrated that the temperature at which a characteristic kink in $\tau_\alpha(T)$ dependence is observed corresponds to the vitrification of the interfacial layer.[95] However, the enhanced dynamics of molecules confined in AAO nanopores compared to the bulk sample were attempted to explain differently, for example, crossing a spinodal temperature,[96] dynamic exchange between the surface layer and free molecules,[97] frustration in the density,[18,33,47] or approaching the length scale of cooperative dynamics.[25]

Numerous experimental research suggests that the thermal protocol impacts the glass-transition dynamics in nanopores.[30,33,46,96,98,99] With this knowledge, the experiments were executed by using two different thermal protocols. The dielectric results were obtained upon slow cooling from the room temperature with the rate of 0.2 K/min and slow heating from the glassy state with 0.2 K/min following cooling with 10 K/min to low temperatures. The measured temperature dependences of the segmental relaxation time for the studied polymer are presented in the inset of Figure 4a. As can be seen, on cooling, for PMPS 2.5k confined in 55 nm native nanopores, the segmental relaxation time shows the bulk behavior. At the same time, on heating (even in the same temperature range), the characteristic deviation is observed.

On the contrary, the opposite behavior is observed for the studied polymer confined in 50 nm pores with HfO_2 coating. The sample shows no systematic crossover in $\tau_\alpha(T)$ on heating, while on cooling, the segmental dynamics suddenly deviate from the bulk. We have also seen similar effects for PMPS confined within alumina nanopores with the chemically modified surfaces using silane agents (ClTMS and APTMOS) and varying amounts of polar and nonpolar groups attached to the surface.[20,21] Thus, it should be remembered that the segmental relaxation time in confinement might evolve differently, depending on the thermal treatment. Such a feature comes from the confined polymer being in an out-of-equilibrium state. Depending on the time provided, it can restore partially or even completely its bulk segmental relaxation time at a given temperature. The results of our previous investigation demonstrate clearly that the surface chemistry/polarity might control such an equilibration process.[21]

Chat et al. have demonstrated that the glass-transition dynamics do not change with the thermal treatment for dimethyl phthalate confined in 50 nm pores with 5 nm HfO_2 coating.[68] However, for the S-Methoxy-PC confined in AAO nanopores with the same type of ALD coatings, they did not observe a significant deviation of the temperature dependence of the α-relaxation process from bulk behavior.[69] As concluded, such a difference might be explained due to the different sensitivity of both glass-forming systems to pressure effects/density frustration.

Subsequently, we have also investigated changes in the segmental dynamics of the confined polymer as a function of pore diameter. For that purpose, we have varied with the pore size while keeping the same ALD coating, which was SiO_2. The

https://doi.org/10.1021/acs.macromol.2c00311
Macromolecules XXXX, XXX, XXX−XXX

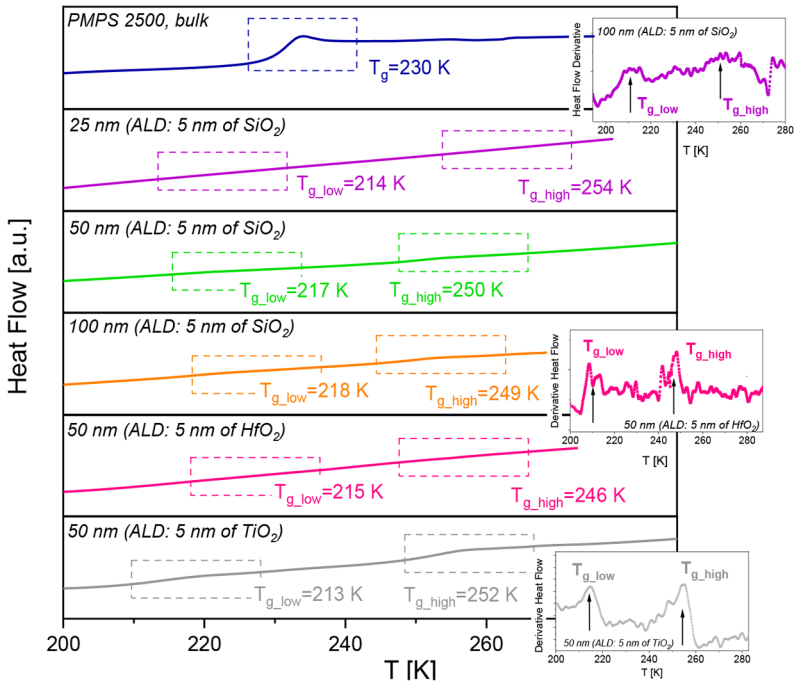

Figure 6. DSC thermograms for PMPS 2.5k in the bulk state and embedded within AAO nanopores with different ALD coatings. DSC scans were recorded on heating at 10 K/min following cooling with 2 K/min. The insets show the temperature derivatives of the heat flow signals for selected samples.

corresponding results are shown in Figure 4b. As can be seen, with decreasing the pore diameter, the deviation from bulk behavior shifts toward higher temperature. So at a given temperature, located below a characteristic kink, the segmental dynamics is enhanced with reducing the pore size. This is a characteristic feature for glass-forming substances under nanoconfinement, reported already in numerous studies.[25,36,47,48,57,58,100−103] As already noted, it turns out that by combining dielectric relaxation and calorimetric studies, the characteristic deviation of $\tau_\alpha(T)$ from the bulk dependence seen in alumina nanopores can be ascribed to vitrification of the molecules in the interfacial layer.[11,58,93]

In the next step, we have investigated the distribution of the α-relaxation time for the PMPS 2.5k confined in cylindrical alumina nanopores with different coating; see results presented in Figure 5a,b. As can be seen, the α-loss peak becomes broader in nanopore confinement. This feature is evident with decreasing the pore diameter. Such spectral broadening is characteristic of geometrically constrained systems and signifies that the dipolar environment becomes more and more heterogeneous.[57,75,89,96,104−109] Some of the literature reports indicate that silanization of the inner pore walls should completely remove the broadening of the α-relaxation peak in nanopore confinement.[52,57] However, in our previous work, we have observed the opposite trend for PMPS 2.5k confined in AAO nanopores with the surface conditions modified by using different silane agents, ClTMS and APTMOS. The confinement effect seen as broadening the α-loss peak was not eliminated by chemical modification. In contrast, it becomes even more pronounced. We have assumed that for APTMOS-treated nanopores, it may be due to the complex properties and specific interfacial interactions between the polymer and APTMOS molecules. For ClTMS and the native pores, we observed that their segmental relaxation time distribution was practically the same. Likewise, the broadening distribution of the segmental relaxation time was not eliminated in AAO nanopores with varying surface polarity.[21] As a matter of fact, the distribution of the α-relaxation times was practically not affected by changes in the surface conditions. Altogether, it was concluded that the changes in the surface chemistry might impact various aspects of the relaxation dynamics in absolutely different ways.[20]

As shown in Figure 5a, the broadening of the α-relaxation changes with the type of ALD coating and the pore size. For 50 nm pores with hydrophobic HfO_2 surfaces, the shape of the α-relaxation peak is broader compared to SiO_2 coatings, which have a more hydrophilic character. This observation shows that a more heterogeneous nature of the relaxation dynamics is expected in pores with hydrophobic surfaces. The same feature was also observed for dimethyl phthalate confined in 50 nm pores with 5 nm HfO_2 coating[68] and for S-Methoxy-PC confined in 25 nm pores with 5 nm HfO_2 coating.[69] Apart from that, it should be noted that the different thermal protocols that we use to collect the dielectric spectra do not affect further changes in the shape of the α-loss peak, as demonstrated in Figure 5b.

We have used the Kohlrausch−Williams−Watts (KWW) stretched exponential to describe the shape of the α-relaxation[110,111]

$$\phi(t) = A \exp\left[-\left(\frac{t}{\tau}\right)^{\beta_{KWW}}\right] \quad (4)$$

where τ_α is the relaxation time and t is time. The value of β_{KWW} varies between 0 and 1. It decreases as the relaxation spectrum broadens. The values obtained for the nanopore-confined polymer are much lower than for the bulk polymer. Such broadening of the α-relaxation in nanopores is a characteristic feature of many glass-forming systems under geometrical confinement. It is often related to the increase of

https://doi.org/10.1021/acs.macromol.2c00311
Macromolecules XXXX, XXX, XXX−XXX

heterogeneous relaxation dynamics. Furthermore, with decreasing pore size, the β_{KWW} value also decreases while it remains unchanged for the different thermal protocols. By comparing the results from the previous study of PMPS 2.5k confined within alumina nanopores with modified surface conditions, we found that the values of the stretching exponents reported when using ClTMS and APTMOS agents are larger than that obtained in AAO templates with controlled surface polarity and ALD coated reported in the present work. For ClTMS-coated pores, we get 0.36, while for the more hydrophilic APTMOS surface, 0.28. In the case of surface polarity changes induced by controlling the separation between polar and nonpolar units, the distribution of the α-relaxation times was practically not affected. All the samples have $\beta_{KWW} \sim 0.21$. On the basis of that finding, we conclude that the breadth of the relaxation function detects to some extent changes in the surface conditions. Our present results also support that finding. We observe apparent differences in the distribution of the relaxation times for PMPS confined within 50 nm AAO templates with HfO_2 and SiO_2 coatings. As will be demonstrated in the following part of this paper, we also found surprisingly low polymer−substrate interfacial energy values in the former system; in contrast, for the latter, the polymer−substrate interfacial energy is very high.

To complement dielectric relaxation studies, we have also performed calorimetric measurements. The collected results for PMPS 2.5k in bulk and confined AAO nanopores with the different ALD coatings are presented in Figure 6. In some thermograms recorded for the confined polymer, the step characteristic for the T_g value can be difficult to perceive. For this reason, to confirm the presence of both glass transition events, we have also calculated the temperature derivatives of the heat flow curves, as demonstrated in the inset of Figure 6. Now, it is clearer that the two intense peaks correspond to two glass transition events. The same procedure was repeated for other samples. In all confined samples, two glass-transition temperatures were evident.

The collected DSC results indicate that we can distinguish only one endothermic event resulting from the vitrification process (T_g = 230 K). On the other hand, two glass transition events are detected for PMPS 2.5k confined in alumina nanopores with different ALD coatings. The first glass transition event, seen at lower temperatures, T_{g_low}, is typically assigned with the glass transition of the molecules in the center of the pores. In contrast, the glass transition seen at higher temperatures, T_{g_high}, might be related to the vitrification of the interfacial layer. Such terminology is often recalled as a two-layer model and was already reported in the literature.[30,31,37,46,58,96,99] The values of T_{g_high} and T_{g_low} were determined to be the approximate midpoints of the temperature range over which the glass transition events occur. The accuracy of T_g determination varies within ±3 K. As illustrated in Figure 6, with decreasing the pore size T_{g_low} values slightly decrease, while T_{g_high} values increase. For example, a similar trend was reported in van der Waals-bonded molecular liquids confined to alumina nanopores.[112] Furthermore, by comparing the values of T_{g_high} and T_{g_low} for PMPS 2.5k embedded within alumina nanopores with different ALD coatings, we can see changes in the hydrophobicity/hydrophilicity of the surface do not have a definite impact on T_g values.

We can find that they barely coincide by comparing values corresponding to a characteristic crossover temperature in $\tau_\alpha(T)$ dependence and T_{g_high}. However, does it explicitly mean that changes in $\tau_\alpha(T)$ are due to vitrification of the interfacial layer? Or, in other words, how certain is that T_{g_high} seen in DSC results comes from the vitrification of the interfacial layer? As already noted, numerous experimental results reported in the literature confirmed this kind of behavior for different glass-forming substances under confinement.[22,56,58,93,99,108,113] Many of them, indeed, associate the presence of T_{g_high} with the interfacial layer. This essentially should not raise any doubts when considering native alumina nanopores full of hydrogen-bonded surface OH groups, so capable of forming hydrogen bonding with the confined material.

When it comes to chemically modified pore walls, the interfacial interactions are expected to be either weakened or strengthened, depending on the surface modification strategy. Changes in the dynamics of the interfacial layer induced in this way should be immediately reflected in changes of high T_g value. In principle, in the absence of interfacial interactions, T_{g_high} should not be observed. Herein, it should be noted that in our previous works the two-glass transition event was also revealed upon calorimetric measurement of nanopore-confined PMPS 2.5k, irrespective of the chemical modification strategy used.[20,21]

However, the presence of both T_gs can also be detected in the case of a complete lack of strong H-bonding and surface interactions. To demonstrate that, we have calculated interfacial energy, which provides information about the strength of the interactions between the polymer and constrained solid surface. The details of the calculation procedure can be found in the Supporting Information. The results lead to the following values: γ_{SL} = 18.7 mN/m for PMPS 2.5k confined in AAO nanopores with SiO_2 coating, γ_{SL} = 5.1 mN/m for TiO_2 coating, and γ_{SL} = 0.5 for HfO_2 coating (values calculated by using water and formamide as pair test liquids). As can be seen, PMPS 2.5k confined to AAO nanopores with the most hydrophobic HfO_2 coating is characterized by extremely low interfacial energy, while for the SiO_2-coated system, the interfacial energy is considerable. This indicates that nanopore confined PMPS 2.5k weakly wets and interacts with HfO_2-coated pore walls, while in the presence of SiO_2 coatings, the polymer/solid substrate interactions are stronger. Despite that, we still observe two glass-transition events in DSC thermograms in both cases. In the literature, the change in T_g under confinement was discussed in the context of interfacial energy.[51,75] Namely, a trend for a decreasing glass temperature relative to the bulk with increasing interfacial energy was observed. While it is a valuable general finding reported for numerous glass-forming liquids and polymers, it does not apply when it comes to a detailed analysis of a single system confined within a nanoporous matrix of different surface properties. In Figure 7, we plot on the same graph T_{g_high}, T_{g_low}, and γ_{SL} gathered for the investigated samples. As can be seen, the values of high and low glass transition temperatures practically do not depend on the interfacial energy value. Compared with the bulk polymer, a downward shift of T_g will be practically the same, $\Delta T \sim 15 \pm 2$ K.

Another point should be noted here. Talik and co-workers reported glycerol confined within alumina nanopores with no confinement effect. The presence of only one glass-transition temperature, corresponding to the bulk value, was related to the very low interfacial energy γ_{SL} = 1.5 mN/m of this system.[51] It was also suggested that good wettability and strong

https://doi.org/10.1021/acs.macromol.2c00311
Macromolecules XXXX, XXX, XXX−XXX

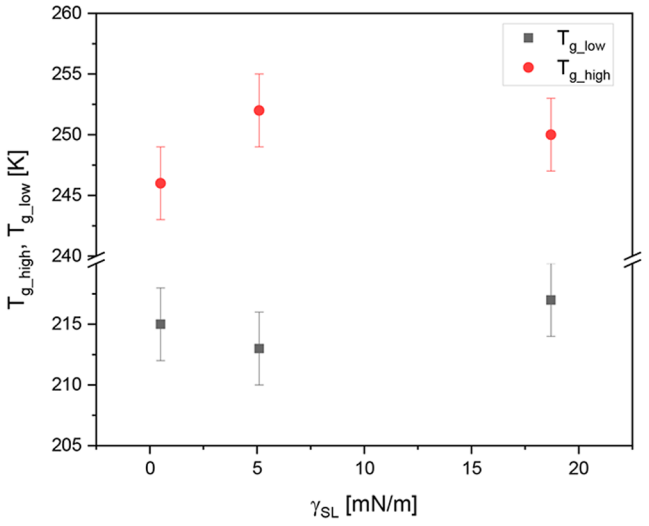

Figure 7. Interfacial energy for PMPS 2.5k confined within 50 nm AAO nanopores with different ALD coatings plotted as a function of high and low glass-transition temperatures determined from the calorimetric measurements.

interactions with the substrate are the two most important parameters responsible for the formation of a stable interfacial layer. This is again not valid in our case, raising an open question on whether a high T_g value is indeed related to the presence of the so-called "interfacial" layer.

Recently, Wang and co-workers[114] discussed the relation between conformational changes induced in confinement and T_g. Although the system under investigation has minimal interfacial interactions, the authors have reported dramatic changes in T_g behavior depending on whether concave or convex geometry was used. This feature was related to molecular conformation changes controlled by the molecular packing of the molecules. To get new information about conformational and structural changes induced in confinement, we have also performed a Raman spectroscopy study for the tested polymer confined in AAO templates with different ALD coatings. The detailed analysis of collected Raman spectra can be found in the Supporting Information. The most important outcome from this study is that nanometric confinement results in two main features: symmetry breaking within the siloxane backbone and alterations in the benzene ring alignment. The particular changes in the surface chemistry can be only responsible for slightly higher structural modifications within siloxane- and aromatic-related bands.

To sum up, in all of the methods that have been employed to modify the surface of alumina nanopores, we still observe two T_gs in DSC spectra of confined PMPS 2.5k. This is a very intriguing finding. In view of the calculated interfacial energy values, we cannot explain it by considering changes in the strength of guest−host interactions. Even in the absence of strong interfacial interactions, high T_g is detected. There is no threshold in γ_{SL}, below which the surface interactions are too weak to induce confinement effect and double glass-transition phenomenon. This points out that some other phenomena might probably occur close to the surface, not considered so far. One possible scenario is related to density variation close to the substrate, as suggested by Wang and co-workers.[114] In this view, in confined material, we can distinguish high- and low-density regions with different T_gs. In the *N*,*N*′-bis(3-methylphenyl)-*N*,*N*′-diphenylbenzidine (TPD) case, studied by Wang et al., the pore curvature promotes itself various molecular packing. However, this is not the case for PMPS 2.5k because, in all of the cases, the pore geometry was the same. Thus, the presence of two T_gs in nanoporous confinement remains unclear. It is generally agreed that understanding how soft matter systems behave close to the solid interfaces is essential to the design of nanometric size interfaces with controlled physical properties and further applications of such systems. This study shows that not all of the features related to glass-transition dynamics of nanopore-confined polymers can be explained by the strength of interfacial interactions. Therefore, a more rigorous and complete understanding of two T_gs in confinement requires further experiments and additional simulations, especially considerable insight into the density distribution and structure is greatly needed.

CONCLUSIONS

In this work, by employing dielectric spectroscopy and differential scanning calorimetry, we have investigated how modification of the surface conditions affects the glass transition dynamics of PMPS 2.5k confined in nanoporous alumina templates. The inner surface of the pores was modified by using the atomic layer deposited technique. Each AAO membrane was covered by 5 nm thick ALD coating of either hafnium oxide (HfO_2), silicon oxide (SiO_2), and titanium oxide (TiO_2). On the basis of contact angle measurements, we have confirmed that HfO_2 coating is responsible for the most hydrophobic surface properties, while SiO_2 and TiO_2 result in a more hydrophilic character of the pore walls. In line with this, the polymer/substrate interfacial energy was extremely low in the case of HfO_2 coatings (0.5 mN/m) and remarkably strong for SiO_2 coating (18.7 mN/m). Therefore, just by changing the ALD coating, we tuned for the same polymer material the interfacial interactions from exceptionally strong to exceptionally weak.

The results of the dielectric studies reveal that for the studied polymer confined in ALD-coated nanopores the α-relaxation time exhibits a strong dependence on the thermal treatment protocol. As a result, in some cases, it was possible to see either enhanced or bulk-like evolution of $\tau_\alpha(T)$. The distribution of the α-relaxation time indicates that the broadening of the α loss peak is more pronounced when we decrease the pore diameter and when the surface has more hydrophobic properties. We note that the broadening of the segmental relaxation peak, which is characteristic for the nanopore-confined systems, is not eliminated by changing the surface chemistry. For all considered systems, the DSC thermograms have revealed the presence of two glass transition events. This observation indicates that irrespective of the surface character, we cannot remove the confinement effect or double glass transition event seen in alumina nanopores. The strength of the interfacial interactions does not relate to changes in T_g behavior of confined PMPS 2.5k. From that it remains an open question on whether by changing the surface characteristics we prevent in any way formation of an interfacial layer between the confined polymer and confining walls or the presence of two glass transition temperatures in calorimetric response of nanopore-confined material is related to some other phenomenon taking place close to the pore surface, such as frustration in the density.

While the strength of the interfacial interactions under geometric confinement was proven many times to play a

https://doi.org/10.1021/acs.macromol.2c00311
Macromolecules XXXX, XXX, XXX−XXX

critical role in understanding the polymers' dynamics at the nanoscale level, this study provides evidence that it failed to explain the double glass transition phenomenon for the tested polymer material embedded within cylindrical nanopores with different surface coating. Our study was designed to show that strong interfacial interactions are not needed to see high T_g. With this, it is evident that there should be some other important factors not taken so far into account. Thus, the presence of double glass-transition event in cylindrical pores remains even more unclear. Further studies, hopefully with the aid of computer simulations, should focus on elucidating the problem encountered for confined PMPS 2.5k. Understanding how the surface properties affect polymer behavior at the nanoscale level should help develop polymer surfaces with controlled physical properties for versatile applications.

■ ASSOCIATED CONTENT

Supporting Information

The Supporting Information is available free of charge at https://pubs.acs.org/doi/10.1021/acs.macromol.2c00311.

Nitrogen adsorption/desorption isotherms measurements, scanning electron microscope results, analysis of the dielectric permittivity for the empty membranes with the correction of the dielectric data for the confined polymer, calculation of the interfacial energy between the investigated polymer and ALD-coated alumina, and a Raman spectroscopy study of conformation and structural changes induced in nanopore confinement (PDF)

■ AUTHOR INFORMATION

Corresponding Authors

Roksana Winkler − *Institute of Physics, University of Silesia, 41-500 Chorzow, Poland; Silesian Center for Education and Interdisciplinary Research (SMCEBI), 41-500 Chorzow, Poland;* orcid.org/0000-0001-8713-4308; Email: rwinker@us.edu.pl

Karolina Adrjanowicz − *Institute of Physics, University of Silesia, 41-500 Chorzow, Poland; Silesian Center for Education and Interdisciplinary Research (SMCEBI), 41-500 Chorzow, Poland;* orcid.org/0000-0003-0212-5010; Email: kadrjano@us.edu.pl

Authors

Katarzyna Chat − *Institute of Physics, University of Silesia, 41-500 Chorzow, Poland; Silesian Center for Education and Interdisciplinary Research (SMCEBI), 41-500 Chorzow, Poland;* orcid.org/0000-0002-6972-2859

Aparna Beena Unni − *Institute of Physics, University of Silesia, 41-500 Chorzow, Poland; Silesian Center for Education and Interdisciplinary Research (SMCEBI), 41-500 Chorzow, Poland;* orcid.org/0000-0001-5073-4537

Mateusz Dulski − *Institute of Materials Engineering, University of Silesia in Katowice, 40-007 Katowice, Poland;* orcid.org/0000-0001-8686-1853

Magdalena Laskowska − *Institute of Nuclear Physics, Polish Academy of Sciences, 31-342 Krakow, Poland*

Lukasz Laskowski − *Institute of Nuclear Physics, Polish Academy of Sciences, 31-342 Krakow, Poland*

Complete contact information is available at: https://pubs.acs.org/10.1021/acs.macromol.2c00311

Notes

The authors declare no competing financial interest.

■ ACKNOWLEDGMENTS

This work was supported by the resources of the National Science Centre [Grant 2017/27/B/ST3/00402 (K.A.) and Grant 2017/26/E/ST5/00162 (Ł.L.)].

■ REFERENCES

(1) Gitsas, A.; Yameen, B.; Lazzara, T. D.; Steinhart, M.; Duran, H.; Knoll, W. Polycyanurate Nanorod Arrays for Optical-Waveguide-Based Biosensing. *Nano Lett.* **2010**, *10*, 2173−2177.

(2) García-Gutiérrez, M.-C.; Linares, A.; Hernández, J. J.; Rueda, D. R.; Ezquerra, T. A.; Poza, P.; Davies, R. J. Confinement-Induced One-Dimensional Ferroelectric Polymer Arrays. *Nano Lett.* **2010**, *10*, 1472−1476.

(3) Lau, K. H. A.; Tan, L.-S.; Tamada, K.; Sander, M. S.; Knoll, W. Highly Sensitive Detection of Processes Occurring Inside Nanoporous Anodic Alumina Templates: A Waveguide Optical Study. *J. Phys. Chem. B* **2004**, *108*, 10812−10818.

(4) Kabashin, A. V.; Evans, P.; Pastkovsky, S.; Hendren, W.; Wurtz, G. A.; Atkinson, R.; Pollard, R.; Podolskiy, V. A.; Zayats, A. V. Plasmonic Nanorod Metamaterials for Biosensing. *Nat. Mater.* **2009**, *8*, 867−871.

(5) Grimm, S.; Giesa, R.; Sklarek, K.; Langner, A.; Gösele, U.; Schmidt, H.-W.; Steinhart, M. Nondestructive Replication of Self-Ordered Nanoporous Alumina Membranes via Cross-Linked Polyacrylate Nanofiber Arrays. *Nano Lett.* **2008**, *8*, 1954−1959.

(6) Li, W. J.; Laurencin, C. T.; Caterson, E. J.; Tuan, R. S.; Ko, F. K. Electrospun Nanofibrous Structure: A Novel Scaffold for Tissue Engineering. *J. Biomed. Mater. Res.* **2002**, *60*, 613−621.

(7) Matthews, J. A.; Wnek, G. E.; Simpson, D. G.; Bowlin, G. L. Electrospinning of Collagen Nanofibers. *Biomacromolecules* **2002**, *3*, 232−238.

(8) Richert, R. Dynamics of Nanoconfined Supercooled Liquids. *Annu. Rev. Phys. Chem.* **2011**, *62*, 65−84.

(9) Kremer, F. *Dynamics in Geometrical Confinement*; Springer: Cham, 2014.

(10) Napolitano, S.; Wübbenhorst, M. The Lifetime of the Deviations from Bulk Behaviour in Polymers Confined at the Nanoscale. *Nat. Commun.* **2011**, *2*, 260.

(11) Tarnacka, M.; Kaminska, E.; Kaminski, K.; Roland, C. M.; Paluch, M. Interplay between Core and Interfacial Mobility and Its Impact on the Measured Glass Transition: Dielectric and Calorimetric Studies. *J. Phys. Chem. C* **2016**, *120*, 7373−7380.

(12) Gin, P.; Jiang, N.; Liang, C.; Taniguchi, T.; Akgun, B.; Satija, S. K.; Endoh, M. K.; Koga, T. Revealed Architectures of Adsorbed Polymer Chains at Solid-Polymer Melt Interfaces. *Phys. Rev. E* **2012**, *109*, 265501.

(13) Minecka, A.; Kaminska, E.; Tarnacka, M.; Talik, A.; Grudzka-Flak, I.; Wolnica, K.; Dulski, M.; Kaminski, K.; Paluch, M. Conformational Changes Underlying Variation in the Structural Dynamics of Materials Confined at the Nanometric Scale. *Phys. Chem. Chem. Phys.* **2018**, *20*, 30200−30208.

(14) Jasiurkowska-Delaporte, M.; Kossack, W.; Kipnusu, W. K.; Sangoro, J. R.; Iacob, C.; Kremer, F. Glassy Dynamics of Two Poly(Ethylene Glycol) Derivatives in the Bulk and in Nanometric Confinement as Reflected in Its Inter- and Intra-Molecular Interactions. *J. Chem. Phys.* **2018**, *149*, 064501.

(15) White, R. P.; Lipson, J. E. G. Connecting Pressure-Dependent Dynamics to Dynamics under Confinement: The Cooperative Free Volume Model Applied to Poly(4-Chlorostyrene) Bulk and Thin Films. *Macromolecules* **2018**, *51*, 7924−7941.

(16) Napolitano, S.; Rotella, C.; Wübbenhorst, M. Can Thickness and Interfacial Interactions Univocally Determine the Behavior of Polymers Confined at the Nanoscale? *ACS Macro Lett.* **2012**, *1*, 1189−1193.

(17) Tarnacka, M.; Kipnusu, W. K.; Kaminska, E.; Pawlus, S.; Kaminski, K.; Paluch, M. The Peculiar Behavior of the Molecular Dynamics of a Glass-Forming Liquid Confined in Native Porous Materials - the Role of Negative Pressure. *Phys. Chem. Chem. Phys.* **2016**, *18*, 23709−23714.
(18) Adrjanowicz, K.; Kaminski, K.; Koperwas, K.; Paluch, M. Negative Pressure Vitrification of the Isochorically Confined Liquid in Nanopores. *Phys. Rev. Lett.* **2015**, *115*, 265702.
(19) Tarnacka, M.; Wojtyniak, M.; Brzózka, A.; Talik, A.; Hachuła, B.; Kamińska, E.; Sulka, G. D.; Kaminski, K.; Paluch, M. Unique Behavior of Poly(Propylene Glycols) Confined within Alumina Templates Having a Nanostructured Interface. *Nano Lett.* **2020**, *20*, 5714−5719.
(20) Winkler, R.; Tu, W.; Laskowski, L.; Adrjanowicz, K. Effect of Surface Chemistry on the Glass-Transition Dynamics of Poly(Phenyl Methyl Siloxane) Confined in Alumina Nanopores. *Langmuir* **2020**, *36*, 7553−7565.
(21) Winkler, R.; Tu, W.; Dulski, M.; Laskowski, L.; Adrjanowicz, K. Effect of the Surface Polarity, Through Employing Nonpolar Spacer Groups, on the Glass-Transition Dynamics of Poly(Phenyl Methylsiloxane) Confined in Alumina Nanopores. *Macromolecules* **2021**, *54*, 10951−10968.
(22) Jackson, C. L.; McKenna, G. B. The Glass Transition of Organic Liquids Confined to Small Pores. *J. Non-Cryst. Solids* **1991**, *131*−*133*, 221−224.
(23) Morineau, D.; Xia, Y.; Alba-Simionesco, C. Finite-Size and Surface Effects on the Glass Transition of Liquid Toluene Confined in Cylindrical Mesopores. *J. Chem. Phys.* **2002**, *117*, 8966−8972.
(24) Blaszczyk-Lezak, I.; Hernández, M.; Mijangos, C. One Dimensional PMMA Nanofibers from AAO Templates. Evidence of Confinement Effects by Dielectric and Raman Analysis. *Macromolecules* **2013**, *46*, 4995−5002.
(25) Arndt, M.; Stannarius, R.; Groothues, H.; Hempel, E.; Kremer, F. Length Scale of Cooperativity in the Dynamic Glass Transition. *Phys. Rev. Lett.* **1997**, *79*, 2077−2080.
(26) Alexandris, S.; Sakellariou, G.; Steinhart, M.; Floudas, G. Dynamics of Unentangled Cis −1,4-Polyisoprene Confined to Nanoporous Alumina. *Macromolecules* **2014**, *47*, 3895−3900.
(27) Zhang, J.; Liu, G.; Jonas, J. Effects of Confinement on the Glass Transition Temperature of Molecular Liquids. *J. Phys. Chem.* **1992**, *96*, 3478−3480.
(28) Schönhals, A.; Goering, H.; Schick, C.; Frick, B.; Zorn, R. Glass Transition of Polymers Confined to Nanoporous Glasses. *Colloid & Polymer Science* **2004**, *282*, 882−891.
(29) Shin, K.; Obukhov, S.; Chen, J.-T.; Huh, J.; Hwang, Y.; Mok, S.; Dobriyal, P.; Thiyagarajan, P.; Russell, T. P. Enhanced Mobility of Confined Polymers. *Nat. Mater.* **2007**, *6*, 961−965.
(30) Tarnacka, M.; Dulski, M.; Geppert-Rybczyńska, M.; Talik, A.; Kamińska, E.; Kamiński, K.; Paluch, M. Variation in the Molecular Dynamics of DGEBA Confined within AAO Templates above and below the Glass-Transition Temperature. *J. Phys. Chem. C* **2018**, *122*, 28033−28044.
(31) Tarnacka, M.; Madejczyk, O.; Kaminski, K.; Paluch, M. Time and Temperature as Key Parameters Controlling Dynamics and Properties of Spatially Restricted Polymers. *Macromolecules* **2017**, *50*, 5188−5193.
(32) Tarnacka, M.; Kaminski, K.; Mapesa, E. U.; Kaminska, E.; Paluch, M. Studies on the Temperature and Time Induced Variation in the Segmental and Chain Dynamics in Poly(Propylene Glycol) Confined at the Nanoscale. *Macromolecules* **2016**, *49*, 6678−6686.
(33) Adrjanowicz, K.; Paluch, M. Discharge of the Nanopore Confinement Effect on the Glass Transition Dynamics via Viscous Flow. *Phys. Rev. Lett.* **2019**, *122*, 176101.
(34) Jackson, C. L.; McKenna, G. B. Vitrification and Crystallization of Organic Liquids Confined to Nanoscale Pores. *Chem. Mater.* **1996**, *8*, 2128−2137.
(35) Alcoutlabi, M.; McKenna, G. B. Effects of Confinement on Material Behaviour at the Nanometre Size Scale. *J. Phys.: Condens. Matter* **2005**, *17*, R461−R524.
(36) Kremer, F.; Huwe, A.; Schönhals, A.; Różański, S. A. Molecular Dynamics in Confining Space. In *Broadband Dielectric Spectroscopy*; Springer: Berlin, 2003; pp 171−224.
(37) Park, J.-Y. Y.; McKenna, G. B. Size and Confinement Effects on the Glass Transition Behavior of Polystyrene/ o -Terphenyl Polymer Solutions. *Physical Review B - Condensed Matter and Materials Physics* **2000**, *61*, 6667−6676.
(38) Kremer, F.; Schönhals, A.; Volkov, A. A.; Prokhorov, A. S.; Kremer, F.; Schönhals, A. In *Broadband Dielectric Spectroscopy*; Kremer, F., Schönhals, A., Eds.; Springer: Berlin, 2003; Vol. *46*.
(39) Napolitano, S. *Non-Equilibrium Phenomena in Confined Soft Matter: Irreversible Adsorption, Physical Aging and Glass Transition at the Nanoscale*; Springer: 2015.
(40) Rotella, C.; Napolitano, S.; Vandendriessche, S.; Valev, V. K.; Verbiest, T.; Larkowska, M.; Kucharski, S.; Wübbenhorst, M. Adsorption Kinetics of Ultrathin Polymer Films in the Melt Probed by Dielectric Spectroscopy and Second-Harmonic Generation. *Langmuir* **2011**, *27*, 13533−13538.
(41) Rotella, C.; Wübbenhorst, M.; Napolitano, S. Probing Interfacial Mobility Profiles via the Impact of Nanoscopic Confinement on the Strength of the Dynamic Glass Transition. *Soft Matter* **2011**, *7*, 5260−5266.
(42) Serghei, A.; Kremer, F. Metastable States of Glassy Dynamics, Possibly Mimicking Confinement-Effects in Thin Polymer Films. *Macromol. Chem. Phys.* **2008**, *209*, 810−817.
(43) Napolitano, S.; Capponi, S.; Vanroy, B. Glassy Dynamics of Soft Matter under 1D Confinement: How Irreversible Adsorption Affects Molecular Packing, Mobility Gradients and Orientational Polarization in Thin Films. *Eur. Phys. J. E* **2013**, *36*, 61.
(44) Perez-de-Eulate, N. G.; Sferrazza, M.; Cangialosi, D.; Napolitano, S. Irreversible Adsorption Erases the Free Surface Effect on the Tg of Supported Films of Poly(4- Tert -Butylstyrene). *ACS Macro Lett.* **2017**, *6*, 354−358.
(45) Napolitano, S.; Sferrazza, M. How Irreversible Adsorption Affects Interfacial Properties of Polymers. In *Advances in Colloid Interface Science*; Elsevier B.V.: 2017; pp 172−177.
(46) Zhang, C.; Li, L.; Wang, X.; Xue, G. Stabilization of Poly(Methyl Methacrylate) Nanofibers with Core-Shell Structures Confined in AAO Templates by the Balance between Geometric Curvature, Interfacial Interactions, and Cooling Rate. *Macromolecules* **2017**, *50*, 1599−1609.
(47) Kipnusu, W. K.; Elsayed, M.; Kossack, W.; Pawlus, S.; Adrjanowicz, K.; Tress, M.; Mapesa, E. U.; Krause-Rehberg, R.; Kaminski, K.; Kremer, F. Confinement for More Space: A Larger Free Volume and Enhanced Glassy Dynamics of 2-Ethyl-1-Hexanol in Nanopores. *J. Phys. Chem. Lett.* **2015**, *6*, 3708−3712.
(48) Kipnusu, W. K.; Elsayed, M.; Krause-Rehberg, R.; Kremer, F. Glassy Dynamics of Polymethylphenylsiloxane in One- and Two-Dimensional Nanometric Confinement - A Comparison. *J. Chem. Phys.* **2017**, *146*, 203302.
(49) Reid, D. K.; Alves Freire, M.; Yao, H.; Sue, H.-J.; Lutkenhaus, J. L. The Effect of Surface Chemistry on the Glass Transition of Polycarbonate Inside Cylindrical Nanopores. *ACS Macro Lett.* **2015**, *4*, 151−154.
(50) Iacob, C.; Runt, J. Charge Transport of Polyester Ether Ionomers in Unidirectional Silica Nanopores. *ACS Macro Lett.* **2016**, *5*, 476−480.
(51) Talik, A.; Tarnacka, M.; Geppert-Rybczynska, M.; Minecka, A.; Kaminska, E.; Kaminski, K.; Paluch, M. Impact of the Interfacial Energy and Density Fluctuations on the Shift of the Glass-Transition Temperature of Liquids Confined in Pores. *J. Phys. Chem. C* **2019**, *123*, 5549−5556.
(52) Kipnusu, W. K.; Elmahdy, M. M.; Elsayed, M.; Krause-Rehberg, R.; Kremer, F. Counterbalance between Surface and Confinement Effects As Studied for Amino-Terminated Poly(Propylene Glycol) Constraint in Silica Nanopores. *Macromolecules* **2019**, *52*, 1864−1873.
(53) Brás, A. R.; Dionísio, M.; Schönhals, A. Confinement and Surface Effects on the Molecular Dynamics of a Nematic Mixture

https://doi.org/10.1021/acs.macromol.2c00311
Macromolecules XXXX, XXX, XXX−XXX

Investigated by Dielectric Relaxation Spectroscopy. *J. Phys. Chem. B* **2008**, *112*, 8227−8235.
(54) Gainaru, C.; Schildmann, S.; Böhmer, R. Surface and Confinement Effects on the Dielectric Relaxation of a Monohydroxy Alcohol. *J. Chem. Phys.* **2011**, *135*, 174510.
(55) Richert, R.; Yang, M. Surface Induced Glass Transition in a Confined Molecular Liquid. *J. Phys. Chem. B* **2003**, *107*, 895−898.
(56) Szklarz, G.; Adrjanowicz, K.; Tarnacka, M.; Pionteck, J.; Paluch, M. Confinement-Induced Changes in the Glassy Dynamics and Crystallization Behavior of Supercooled Fenofibrate. *J. Phys. Chem. C* **2018**, *122*, 1384−1395.
(57) Arndt, M.; Stannarius, R.; Gorbatschow, W.; Kremer, F. Dielectric Investigations of the Dynamic Glass Transition in Nanopores. *Phys. Rev. E* **1996**, *54*, 5377−5390.
(58) Adrjanowicz, K.; Kolodziejczyk, K.; Kipnusu, W. K.; Tarnacka, M.; Mapesa, E. U.; Kaminska, E.; Pawlus, S.; Kaminski, K.; Paluch, M. Decoupling between the Interfacial and Core Molecular Dynamics of Salol in 2D Confinement. *J. Phys. Chem. C* **2015**, *119*, 14366−14374.
(59) Li, M.; Wu, H.; Huang, Y.; Su, Z. Effects of Temperature and Template Surface on Crystallization of Syndiotactic Polystyrene in Cylindrical Nanopores. *Macromolecules* **2012**, *45*, 5196−5200.
(60) Iacob, C.; Sangoro, J. R.; Papadopoulos, P.; Schubert, T.; Naumov, S.; Valiullin, R.; Kärger, J.; Kremer, F. Charge Transport and Diffusion of Ionic Liquids in Nanoporous Silica Membranes. *Phys. Chem. Chem. Phys.* **2010**, *12*, 13798−13803.
(61) Kipnusu, W. K.; Kossack, W.; Iacob, C.; Jasiurkowska, M.; Rume Sangoro, J.; Kremer, F. Molecular Order and Dynamics of Tris(2-Ethylhexyl)Phosphate Confined in Uni-Directional Nanopores. *Zeitschrift für Physikalische Chemie* **2012**, *226*, 797−805.
(62) Laeri, F.; Schüth, F.; Simon, U.; Wark, M. In *Host-Guest-Systems Based on Nanoporous Crystals*; Laeri, F., Schüth, F., Simon, U., Wark, M., Eds.; Wiley-VCH: Weinheim, 2003.
(63) Iacob, C.; Sangoro, J. R.; Kipnusu, W. K.; Valiullin, R.; Kärger, J.; Kremer, F. Enhanced Charge Transport in Nano-Confined Ionic Liquids. *Soft Matter* **2012**, *8*, 289−293.
(64) Sha, Y.; Li, L.; Wang, X.; Wan, Y.; Yu, J.; Xue, G.; Zhou, D. Growth of Polymer Nanorods with Different Core-Shell Dynamics via Capillary Force in Nanopores. *Macromolecules* **2014**, *47*, 8722−8728.
(65) Elam, J. W.; Routkevitch, D.; Mardilovich, P. P.; George, S. M. Conformal Coating on Ultrahigh-Aspect-Ratio Nanopores of Anodic Alumina by Atomic Layer Deposition. *Chem. Mater.* **2003**, *15*, 3507−3517.
(66) Stair, P. C.; Marshall, C.; Xiong, G.; Feng, H.; Pellin, M. J.; Elam, J. W.; Curtiss, L.; Iton, L.; Kung, H.; Kung, M.; et al. Novel, Uniform Nanostructured Catalytic Membranes. *Top. Catal.* **2006**, *39*, 181−186.
(67) Xiong, G.; Elam, J. W.; Feng, H.; Han, C. Y.; Wang, H.-H.; Iton, L. E.; Curtiss, L. A.; Pellin, M. J.; Kung, M.; Kung, H.; et al. Effect of Atomic Layer Deposition Coatings on the Surface Structure of Anodic Aluminum Oxide Membranes. *J. Phys. Chem. B* **2005**, *109*, 14059−14063.
(68) Chat, K.; Tu, W.; Beena Unni, A.; Geppert-Rybczyńska, M.; Adrjanowicz, K. Study on the Glass Transition Dynamics and Crystallization Kinetics of Molecular Liquid, Dimethyl Phthalate, Confined in Anodized Aluminum Oxide (AAO) Nanopores with Atomic Layer Deposition (ALD) Coatings. *J. Mol. Liq.* **2020**, *311*, 113296.
(69) Chat, K.; Tu, W.; Laskowski, L.; Adrjanowicz, K. Effect of Surface Modification on the Glass Transition Dynamics of Highly Polar Molecular Liquid S-Methoxy-PC Confined in Anodic Aluminum Oxide Nanopores. *J. Phys. Chem. C* **2019**, *123*, 13365−13376.
(70) Tu, W.; Ngai, K. L.; Paluch, M.; Adrjanowicz, K. Dielectric Study on the Well-Resolved Sub-Rouse and JG β-Relaxations of Poly(Methylphenylsiloxane) at Ambient and Elevated Pressures. *Macromolecules* **2020**, *53*, 1706−1715.
(71) Kriegs, H.; Meier, G.; Gapinski, J.; Patkowski, A. The Effect of Intramolecular Relaxations on the Damping of Longitudinal and Transverse Phonons in Polysiloxanes Studied by Brillouin Spectroscopy. *J. Chem. Phys.* **2008**, *128*, 014507.
(72) Paluch, M.; Casalini, R.; Patkowski, A.; Pakula, T.; Roland, C. M. Effect of Volume Changes on Segmental Relaxation in Siloxane Polymers. *Phys. Rev. E* **2003**, *68*, 5.
(73) Boese, D.; Momper, B.; Meier, G.; Kremer, F.; Hagenah, J. U.; Fischer, E. W. Molecular Dynamics in Poly(Methylphenylsiloxane) As Studied by Dielectric Relaxation Spectroscopy and Quasielastic Light Scattering. *Macromolecules* **1989**, *22*, 4416−4421.
(74) Adrjanowicz, K.; Winkler, R.; Chat, K.; Duarte, D. M.; Tu, W.; Unni, A. B.; Paluch, M.; Ngai, K. L. Study of Increasing Pressure and Nanopore Confinement Effect on the Segmental, Chain, and Secondary Dynamics of Poly(Methylphenylsiloxane). *Macromolecules* **2019**, *52*, 3763−3774.
(75) Alexandris, S.; Papadopoulos, P.; Sakellariou, G.; Steinhart, M.; Butt, H.-J. J.; Floudas, G. Interfacial Energy and Glass Temperature of Polymers Confined to Nanoporous Alumina. *Macromolecules* **2016**, *49*, 7400−7414.
(76) Tu, W.; Jurkiewicz, K.; Adrjanowicz, K. Confinement of Pyrrolidinium-Based Ionic Liquids [CnMPyrr]+[Tf2N]- with Long Cationic Alkyl Side Chains (n = 10 and 16) to Nanoscale Pores: Dielectric and Calorimetric Studies. *J. Mol. Liq.* **2021**, *324*, 115115.
(77) Tu, W.; Chat, K.; Szklarz, G.; Laskowski, L.; Grzybowska, K.; Paluch, M.; Richert, R.; Adrjanowicz, K. Dynamics of Pyrrolidinium-Based Ionic Liquids under Confinement. II. The Effects of Pore Size, Inner Surface, and Cationic Alkyl Chain Length. *J. Phys. Chem. C* **2020**, *124*, 5395−5408.
(78) Richert, R. Comment on "Hidden Slow Dynamics in Water. *Phys. Rev. Lett.* **2010**, *104*, 249801.
(79) Paluch, M.; Pawlus, S.; Kaminski, K. Comment on "Slow Debye-Type Peak Observed in the Dielectric Response of Polyalcohols" [*J. Chem. Phys. 132*, 044504 (**2010**)]. *J. Chem. Phys.* **2011**, *134*, 037101.
(80) Tarnacka, M.; Geppert-Rybczynska, M.; Dulski, M.; Grelska, J.; Jurkiewicz, K.; Grzybowska, K.; Kaminski, K.; Paluch, M. Local Structure and Molecular Dynamics of Highly Polar Propylene Carbonate Derivative Infiltrated within Alumina and Silica Porous Templates. *J. Chem. Phys.* **2021**, *154*, 064701.
(81) Williams, R.; Goodman, A. M. Wetting of Thin Layers of SiO 2 by Water. *Appl. Phys. Lett.* **1974**, *25*, 531−532.
(82) Mills, A.; Crow, M. A Study of Factors That Change the Wettability of Titania Films. *International Journal of Photoenergy* **2008**, *2008*, 1−6.
(83) Santos, F. de P.; Campos, E. de; Costa, M.; Melo, F. C. L.; Honda, R. Y.; Mota, R. P. Superficial Modifications in TiO_2 and Al2O3 Ceramics. *Mater. Res.* **2003**, *6*, 353−357.
(84) Jain, R. K.; Gautam, Y. K.; Dave, V.; Chawla, A. K.; Chandra, R. A Study on Structural, Optical and Hydrophobic Properties of Oblique Angle Sputter Deposited HfO 2 Films. *Appl. Surf. Sci.* **2013**, *283*, 332−338.
(85) Zenkin, S.; Belosludtsev, A.; Kos, Š.; Čerstvý, R.; Haviar, S.; Netrvalová, M. Thickness Dependent Wetting Properties and Surface Free Energy of HfO2 Thin Films. *Appl. Phys. Lett.* **2016**, *108*, 231602.
(86) Zenkin, S.; Kos, Š.; Musil, J. Hydrophobicity of Thin Films of Compounds of Low-Electronegativity Metals. *J. Am. Ceram. Soc.* **2014**, *97*, 2713−2717.
(87) Chen, X.; Mao, S. S. Titanium Dioxide Nanomaterials: Synthesis, Properties, Modifications and Applications. *Chem. Rev.* **2007**, *107*, 2891−2959.
(88) Havriliak, S.; Negami, S. A Complex Plane Representation of Dielectric and Mechanical Relaxation Processes in Some Polymers. *Polymer.* **1967**, *8*, 161−210.
(89) Kremer, F.; Schönhals, A. *Broadband Dielectric Spectroscopy*; Springer: Berlin, 2003.
(90) Vogel, H. The Law of the Relation between the Viscosity of Liquids and the Temperature. *Phys. Z.* **1921**, *22*, 645−646.
(91) Fulcher, G. S. Analysis of Recent Measurements of the Viscosity of Glasses. *J. Am. Ceram. Soc.* **1925**, *8*, 339−355.

https://doi.org/10.1021/acs.macromol.2c00311
Macromolecules XXXX, XXX, XXX−XXX

(92) Tammann, G.; Hesse, W. Die Abhängigkeit Der Viscosität von Der Temperatur Bie Unterkühlten Flüssigkeiten. *Zeitschrift für anorganische und allgemeine Chemie* **1926**, *156*, 245−257.
(93) Adrjanowicz, K.; Kaminski, K.; Tarnacka, M.; Szklarz, G.; Paluch, M. Predicting Nanoscale Dynamics of a Glass-Forming Liquid from Its Macroscopic Bulk Behavior and Vice Versa. *J. Phys. Chem. Lett.* **2017**, *8*, 696−702.
(94) Napolitano, S.; Glynos, E.; Tito, N. B. Glass Transition of Polymers in Bulk, Confined Geometries, and near Interfaces. *Rep. Prog. Phys.* **2017**, *80*, 036602.
(95) Adrjanowicz, K.; Kolodziejczyk, K.; Kipnusu, W. K.; Tarnacka, M.; Mapesa, E. U.; Kaminska, E.; Pawlus, S.; Kaminski, K.; Paluch, M. Decoupling between the Interfacial and Core Molecular Dynamics of Salol in 2D Confinement. *J. Phys. Chem. C* **2015**, *119*, 14366−14374.
(96) Politidis, C.; Alexandris, S.; Sakellariou, G.; Steinhart, M.; Floudas, G. Dynamics of Entangled Cis −1,4-Polyisoprene Confined to Nanoporous Alumina. *Macromolecules* **2019**, *52*, 4185−4195.
(97) Stannarius, R.; Kremer, F.; Arndt, M. Dynamic Exchange Effects in Broadband Dielectric Spectroscopy. *Phys. Rev. Lett.* **1995**, *75*, 4698−4701.
(98) Zhang, C.; Sha, Y.; Zhang, Y.; Cai, T.; Li, L.; Zhou, D.; Wang, X.; Xue, G. Nanostructures and Dynamics of Isochorically Confined Amorphous Drug Mediated by Cooling Rate, Interfacial, and Intermolecular Interactions. *J. Phys. Chem. B* **2017**, *121*, 10704−10716.
(99) Li, L.; Zhou, D.; Huang, D.; Xue, G. Double Glass Transition Temperatures of Poly(Methyl Methacrylate) Confined in Alumina Nanotube Templates. *Macromolecules* **2014**, *47*, 297−303.
(100) Wübbenhorst, M.; Simone, N.; Napolitano, S. Deviations from Bulk Glass Transition Dynamics of Small Molecule Glass Formers: Some Scenarios in Relation to the Dimensionality of the Confining Geometry. *Dynamics in Geometrical Confinement, Advances in Dielectrics* **2014**, 247−277.
(101) Mijangos, C.; Martínez, G.; Millán, J.-L. Dependence of Glass-transition Temperature *Tg* on Tacticity of Poly(Vinyl Chloride). A Preliminary Study by Differential Scanning Calorimetry. *Makromol. Chem.* **1988**, *189*, 567−572.
(102) Brás, A. R.; Fonseca, I. M.; Dionísio, M.; Schönhals, A.; Affouard, F.; Correia, N. T. Influence of Nanoscale Confinement on the Molecular Mobility of Ibuprofen. *J. Phys. Chem. C* **2014**, *118*, 13857−13868.
(103) Wagner, H.; Richert, R. Dielectric Relaxation of the Electric Field in Poly(Vinyl Acetate): A Time Domain Study in the Range 10−3-106 s. *Polymer* **1997**, *38*, 255−261.
(104) Huwe, A.; Kremer, F.; Behrens, P.; Schwieger, W. Dielectric Investigations of the Dynamic Glass Transition in Nanopores; Molecular Dynamics in Confining Space: From the Single Molecule to the Liquid State. *Phys. Rev. Lett.* **1999**, *82*, 2338.
(105) Schüller, J.; Mel'Nichenko, Y. B.; Richert, R.; Fischer, E. W. Dielectric Studies of the Glass Transition in Porous Media. *Phys. Rev. Lett.* **1994**, *73*, 2224−2227.
(106) Mel'nichenko, Yu. B.; Schüller, J.; Richert, R.; Ewen, B.; Loong, C.-K. Dynamics of Hydrogen-bonded Liquids Confined to Mesopores: A Dielectric and Neutron Spectroscopy Study. *J. Chem. Phys.* **1995**, *103*, 2016−2024.
(107) Pissis, P.; Kyritsis, A.; Daoukaki, D.; Barut, G.; Pelster, R.; Nimtz, G. Dielectric Studies of Glass Transition in Confined Propylene Glycol. *J. Phys.: Condens. Matter* **1998**, *10*, 6205−6227.
(108) Pissis, P.; Daoukaki-Diamanti, D.; Apekis, L.; Christodoulides, C. The Glass Transition in Confined Liquids. *J. Phys.: Condens. Matter* **1994**, *6*, L325−L328.
(109) Kremer, F.; Huwe, A.; Arndt, M.; Behrens, P.; Schwieger, W. How Many Molecules Form a Liquid? *J. Phys.: Condens. Matter* **1999**, *11*, A175−A188.
(110) Kohlrausch, R. Nachtrag Uber Die Elastische Nachwirkung Beim Cocon Und Glasfaden. *Pogg. Ann. Phys. (III)* **1847**, *12*, 393−399.
(111) Williams, G.; Watts, D. C. Non-Symmetrical Dielectric Relaxation Behaviour Arising from a Simple Empirical Decay Function. *Trans. Faraday Soc.* **1970**, *66*, 80−85.
(112) Adrjanowicz, K.; Kaminski, K.; Tarnacka, M.; Szklarz, G.; Paluch, M. Predicting Nanoscale Dynamics of a Glass-Forming Liquid from Its Macroscopic Bulk Behavior and Vice Versa. *J. Phys. Chem. Lett.* **2017**, *8*, 696−702.
(113) Le Quellec, C.; Dosseh, G.; Audonnet, F.; Brodie-Linder, N.; Alba-Simionesco, C.; Häussler, W.; Frick, B. Influence of Surface Interactions on the Dynamics of the Glass Former Ortho-Terphenyl Confined in Nanoporous Silica. *European Physical Journal: Special Topics* **2007**, *141*, 11−18.
(114) Wang, H.; Kearns, K. L.; Zhang, A.; Shamsabadi, A. A.; Jin, Y.; Bond, A.; Hurney, S. M.; Morillo, C.; Fakhraai, Z. Effect of Nanopore Geometry in the Conformation and Vibrational Dynamics of a Highly Confined Molecular Glass. *Nano Lett.* **2021**, *21*, 1778−1784.

https://doi.org/10.1021/acs.macromol.2c00311
Macromolecules XXXX, XXX, XXX−XXX